Physics of Fluids LETTER scitation.org/journal/phf

Boundary condition induced passive chaotic mixing in straight microchannels

Cite as: Phys. Fluids **34**, 051703 (2022); doi: 10.1063/5.0088014
Submitted: 11 February 2022 · Accepted: 22 April 2022 ·
Published Online: 6 May 2022

Habilou Ouro-Koura,[1,2] Ayobami Ogunmolasuyi,[2,3] Othman Suleiman,[2] Isaac Omodia,[2] Jaylah Easter,[2] Yasmin Roye,[2,4] and Kausik S. Das[2,a)]

AFFILIATIONS

[1]Department of Mechanical Engineering, Rensselaer Polytechnic Institute, Troy, New York 12180, USA
[2]University of Maryland Eastern Shore, 1, Backbone Road, Princess Anne, Maryland 21853, USA
[3]Department of Mechanical Engineering, Dartmouth College, Troy, New York 12180, USA
[4]Department of Biomedical Engineering, Pratt School of Engineering, Duke University, Durham, North Carolina 27708, USA

[a)]Author to whom correspondence should be addressed: kdas@umes.edu

ABSTRACT

When fluids flow through straight channels sustained turbulence occurs only at high Reynolds numbers [typically Re $\sim O(1000)$]. It is difficult to mix multiple fluids flowing through a straight channel in the low Reynolds number laminar regime [Re $< O(100)$] because in the absence of turbulence, mixing between the component fluids occurs primarily via the slow molecular diffusion process. This Letter reports a simple way to significantly enhance the low Reynolds number (in our case Re ≤ 10) passive microfluidic flow mixing in a straight microchannel by introducing asymmetric wetting boundary conditions on the floor of the channel. We show experimentally and numerically that by creating carefully chosen two-dimensional hydrophobic slip patterns on the floor of the channels, we can introduce stretching, folding, and/or recirculation in the flowing fluid volume, the essential elements to achieve mixing in the absence of turbulence. We also show that there are two distinctive pathways to produce homogeneous mixing in microchannels induced by the inhomogeneity of the boundary conditions. It can be achieved either by (1) introducing stretching, folding and twisting of fluid volumes, i.e., via a horse-shoe type transformation map, or (2) by creating chaotic advection, achieved through manipulation of the hydrophobic boundary patterns on the floor of the channels. We have also shown that by superposing stretching and folding with chaotic advection, mixing can be optimized in terms of significantly reducing mixing length, thereby opening up new design opportunities for simple yet efficient passive microfluidic reactors.

Microfluidics deals with control and manipulation of small volumes of fluids through channels with characteristic length scales on the order of micrometers, and it exercises precise dynamic control over the flow to study new phenomena occurring in fluids. Microfluidics has the potential to solve some of the grand engineering challenges, such as engineering better medicines, providing access to clean water, and solving energy problems due to its ability to use very small controlled volume of samples and reagents, high resolution separation, and detection with great sensitivity.[1–3] Low manufacturing cost, short timescales for analysis along with high throughput designs using device miniaturization, such as lab-on-a-chip[4] or a reactor-on-a-chip,[5] are other advantages. The application of microfluidics is manyfold, ranging from microelectronics, bioanalysis,[6,7] nanoparticle synthesis, organ in a chip, drug development, testing and controlling multiphase flow,[8–10] optofluidics, acoustofluidic patterning,[11] to detection of a single cell,[12,13] single file diffusion,[14] and even a single molecule.[15]

It is clear that microfluidics offers solutions to a plethora of problems. However, growth of microfluidic technologies to the desired level has been stalled by some serious bottlenecks. Many of the applications of microfluidic chips demand homogeneous mixing of reactants. However, it is difficult to mix component fluids in microchannels spontaneously, thanks to the absence of turbulence in the viscosity dominated laminar flow regimes in the small characteristic length scales. One major bottleneck in developing an efficient microfluidic device is, thus, the difficulty in mixing miscible fluid components homogeneously and spontaneously in a low Reynolds number regime.

In a typical microchannel, cross-section length scale (l) is $\sim$100 μm or less. With small flow rates $U \sim 0.1$ m/s, Reynolds numbers (Re $= Ul\rho/\mu$) are typically of the order of 10 or less, where μ is the

dynamic viscosity ($\sim 10^{-3}$ Pa S) and ρ is the density ($\sim 10^3$ kg/m^3 for water) of the fluid. This means that not only inertia is negligible, but also molecular diffusion is the dominant mechanism of mixing of the component fluids in this regime. However, typical diffusivity (D) of species varies from approximately 10^{-9} m^2/s for small molecules including ions, to 10^{-11} m^2/s for large biomolecules. As a result, mixing timescale (l^2/D) is large (>10 s), and Péclet number ($Pe = Ul/D$), the relative measure of diffusive timescale over advective timescale, is also large (10^4–10^6). The length required to mix via diffusion in a flow, thus, ($l_{mix} = lPe$) typically ranges between tens of centimeters to even in meters! One of the strategies that can be employed to enhance mixing in steady laminar diffusion dominated flow regimes comes through a Smale horseshoe map and/or a baker's map.[16] By effectively decreasing the striation length ($l_{\mathrm{Str}} \to 0$), defined as the length scale over which diffusion acts to homogenize the concentration, these maps transform the space (the flow domain) into itself through successive stretching and folding. In this case, the effective interface area across which diffusion takes place increases exponentially leading to a positive Lyapunov exponent. In other words, this is a route to chaos or a rapid growth in mixing, when the problem is translated into the language of dynamical systems.

The other pathway to achieve mixing in low Reynolds number flow goes through "chaotic advection," where the fluid still associates itself with stretching and folding, on top of flows switching instantaneously from one streamline to another.[17] This mechanism of mixing is observed in blinking flows and can be understood theoretically using a twist map.[18] Although both the transformations can be analyzed rigorously using mathematical concepts of ergodicity and dynamical systems, a practical demonstration of these idealized mathematical models is rather difficult to achieve. Mixing via chaotic advection was first demonstrated in the pioneering work on the Staggered Herringbone Mixer (SHM),[19] where flow transverse to the primary flow direction suitable for chaotic advection was generated by placing three dimensional (3D) patterned ridges on the floor of the channels at oblique angles with respect to the downstream direction of the flow. Mixing length varied linearly with ln(Pe) confirming that the stretching and folding of the volumes grow exponentially with respect to the effective mixing length. In contrast, we take a totally new approach in our work to generate similar transverse flow by creating two-dimensional (2D) anisotropic wetting conditions on the floor of the channels experimentally and numerically. Moreover, we show that this type of enhanced mixing is not limited to just Herringbone type patterns, rather a range of computational fluid dynamics simulations reveal the effects of a range of patterns on the flow behavior and their corresponding mixing mechanisms in simple microfluidic channels.

It is well known that surfaces play a big role in micro and nanoscales because the boundary layer essentially spans the whole cross sections of the channels. Since the ratio of solid–liquid interface area ($A \sim l^2$) in a channel and the volume of fluid ($V \sim l^3$) varies inversely to the characteristic length scale of the system ($\sim 1/l$), in small length scales, such as micro- or nanochannels ($l \to 0$), the effect of boundary conditions become increasingly dominant in this asymptotic regime. In this work, we exploit this fact and report that unlike,[19] where 3D miropatterning involving rather complex fabrication process was needed to achieve chaotic advection, here we have achieved mixing at $\mathrm{Re} \leq 10$ by creating essentially 2D hydrophobic patterns using water-repellant ink dots on the channel floor. To be precise, we have used simple hydrophobic permanent marker ink[20] that contains hydrophobic polymer resin to create these very thin hydrophobic patterns on one of the inner floors of the straight channel. The ratio of the thickness of the polymer films to the height of the channels is <0.02, meaning that the hydrophobic regions are essentially 2D with respect to the height of the channels. These hydrophobic dots create a discontinuous jump in the wall boundary conditions forcing the streamlines to readjust instantaneously while crossing the boundary between no-slip to hydrophobic regions. There is less resistance to flow over the water-repellant regions and the liquid flows faster over them than the no-slip regions on the floor of the channels. Moreover, the hydrophobic patterns constrain the fluid to avoid those regions from sticking to the floor, in turn potentially forcing the fluid to generate a velocity component in the transverse direction. Therefore, depending on the strength of hydrophobicity of the ink invisible ridges can be formed periodically at the locations of the hydrophobic patterns. We hypothesize that because of this anisotropic and abrupt flow resistance change due to the difference in wetting boundary conditions on the floor, the fluid generates an average transverse flow, resulting in twisting and stretching of the fluid volume over the cross section of the channel, or creating counter rotating recirculation zones leading to chaotic advection.

The whole fabrication process of microchannels with anisotropic boundary conditions is quite simple and can be done using well known soft photolithography process with polydimethylsiloxane (PDMS) elastomer. Designs of various microchannels are shown in Fig. 1. To create slip regions on the floor of the channels, we have used an unique and easy technique. Recently, it has been shown that many commercially available permanent marker inks, such as Sharpie® inks, create elastic thin polymer films upon drying on a substrate and exhibit water-repellent hydrophobic behavior.[20] The thickness of these hydrophobic polymer films ranges between a few hundred nanometers to a few micrometers. Taking advantage of this hydrophobic property and easy availability of school-supply permanent markers, we have created slip dots on the floor of the channels by simply putting the dots using an ultrafine Sharpie® marker manually. After the

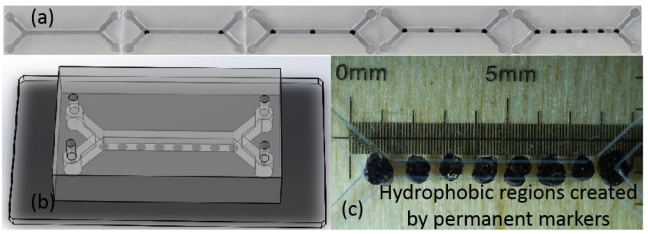

FIG. 1. Designs of straight microchannels with asymmetric boundary condition used in the experiments are shown in these pictures. Dark spots are the hydrophobic regions on the floor of the microchannels. (a) Straight microchannels are made using soft photolithography technique with polydimethylsiloxane (PDMS) elastomer. The first microfluidic chip shows no hydrophobic spot on the floor of the channel. In this case, inlet fluids remain separated as they flow downstream and come out of the outlets. Other microfluidic chips show different number of hydrophobic dots on the floor to enhance mixing. (b) A complete microfluidic chip assembly made by plasma bonding PDMS open channels on a glass slide is shown here. Holes are drilled using a biopsy puncher to connect tubing to the chip. (c) A close-up picture of a microfluidic chip used in the experiments is shown. Hydrophobic dots manually created using a permanent marker are clearly visible through transparent PDMS.

hydrophobic dots are created on a glass slide (Fig. 1), PDMS open channels created by standard soft photolithography process[21] are bonded with the slide using plasma boding techniques.[22,23] The hydrophobic spots created manually on the floor of the channels are not fully symmetrical as expected and can be seen in Fig. 1(c). Several microchannels have been made with width and depth in the range of 100 to 300 μm and the length of the channels in the range of 5–10 mm. In our experiments, Reynolds number is always kept at 10 by controlling the flow speed in the syringe pumps.

Figure 2 shows the schematic of our experiments where two miscible fluids are pumped into the microfluidic reactor through the inlets by two syringe pumps (New Era Pump Systems, NE-1002X) and collected in the cuvette placed at the outlet. The fluids collected at the outlet are analyzed by UV-VIS absorption spectroscopy (Beckman Coulter, DU730) to determine the mixing index and the overall effectiveness of the hydrophobic spots in the mixing of component fluids. In our experiment, we use de-ionized (DI) distilled water (Barnstead NANOpureDiamond water purification system, specific resistivity 18.2 MΩ-cm) in one of the syringe pumps, and DI water mixed with Allura Red dye (Millipore Sigma, D = 3.23 $\times 10^{-10}$ m^2/s, concentration 2 $\times 10^{-5}$ M) in the other. The spectrophotometer was calibrated with pure water with concentration = 0 and with inlet Allura Red solution as 1. In a simple microchannels with usual no-slip inner walls, the output confirms a fully separated flow, i.e., one of the cuvette collects red colored fluid with the same concentration of the input colored fluid, confirmed by the UV-VIS spectroscopic analysis, whereas the other output cuvette collects colorless water. The spectrophotometer is calibrated with a colored solution of known concentration. When the output collected in a cuvette is placed in a UV-VIS spectrometer absorption of light transmitted through the medium becomes directly proportional to the medium concentration. In this case, the fully separated flow through a straight microchannel is characterized by the mixing index 0.5. When a microchannel with hydrophobic marker dots on the floor is used, two input liquids start to mix. To ensure that the adsorption of Allura Red dyes by the marker ink or the dilution of marker ink in water does not affect mixing results, we flush the microchannels with clear, distilled, and de-ionized water for an hour before collecting mixing data. A more direct investigation of the amount of dye adsorbed in the marker dots, if any, can be made by dismantling the microchannels after each experiment, scraping off the marker ink and do elemental analysis of the sample. However, we have not done this analysis in this work. Each experiment is repeated at least five times to ensure reproducibility of the experimental observations. A fully mixed homogeneous fluid's concentration is analyzed by the spectrophotometer, and the mixing index is scaled as 0.

The effect of the slip dots on the degree of mixing at the outlet of the channels, measured experimentally using a spectrophotometer, is shown in Fig. 3. A transition from the laminar separated flow to a homogeneous mixing of component fluids is observed when the number of hydrophobic dots exceeds 3 in a 7 mm channel.

To understand the details of the mixing mechanism, a numerical investigation is done using the finite element simulation software package COMSOL (version 5.4). The bulk flow governed by Navier–Stokes equation $\rho[\frac{\partial \vec{u}}{\partial t} + (\vec{u}\cdot\vec{\nabla})\vec{u}] = -\vec{\nabla}p + \mu\nabla^2\vec{u}$, where $\vec{u}$ is the velocity vector, convection diffusion equations $\frac{\partial c}{\partial t} + (\vec{u}\cdot\vec{\nabla})c = D\nabla^2 c$, where c is the concentration of the fluid, and the continuity equation $\vec{\nabla}\cdot\vec{u} = 0$ is solved. Hydrophobic spots of thickness ~2 μm, similar to experimental marker polymer films,[20] are considered as slip regions ($\vec{u}\cdot\vec{n} = 0$), where $\vec{n}$ is the normal vector at the solid wall boundary with a no-penetration condition. No slip conditions are imposed on the rest of the inner wall regions of the channel by using the condition $\vec{u} = 0$. The steady incompressible flow with laminar outflow and zero outlet static pressure is employed. In the code, Reynolds number is kept at 10 to begin with, to match it with our experimental conditions. However, we have also observed significant mixing in the straight microchannel with patterned hydrophobic regions at lower Re = 1 and Re = 0.1 also.

To further benchmark the code, we first created herringbone type 2D hydrophobic patters on the floor of the channels to mimic the 3D grooved channels in SHM previously reported.[19] It shows similar mixing profiles (Fig. 3 of Ref. 19) in comparison with our simulation results (Fig. 4 of this paper). From the numerical simulations, we have identified two different pathways to achieve homogeneous mixing of component fluids in the low Reynolds number laminar flow regime. Preferential bending of the flow can be achieved by introducing periodic asymmetries in the boundary conditions, created by asymmetric hydrophobic patterns about the centerline of the channel shown in Fig. 5(a). Analogous to the Magnus effect,[24] where difference between the speeds of a fluid flowing over two opposite sides of an object gives rise to a pressure difference in the transverse direction of a flow results in bending of the fluid, here our "duck" shape patterns, for example,

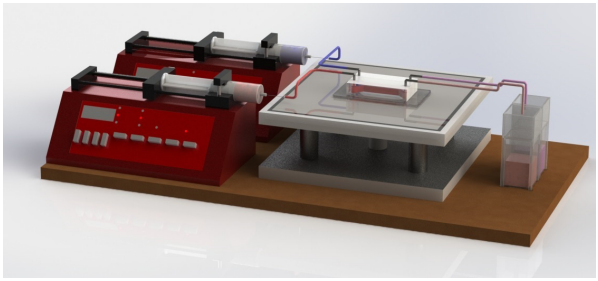

FIG. 2. Schematic of the microfluidic mixing experiment. One of the syringe pumps pushes a colored fluid, and the other brings plain water to the microfluidic chip. Fluid is collected at the outlets after going through the mixer and analyzed by a UV-VIS spectrometers.

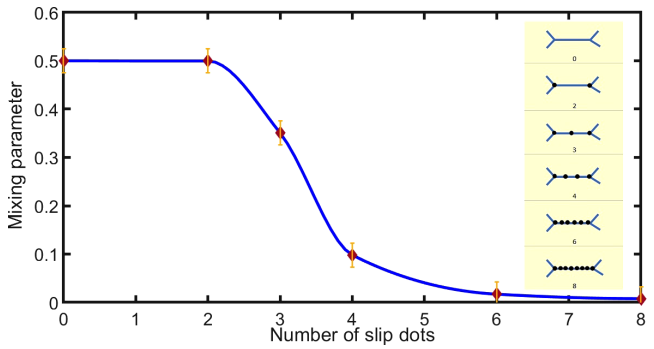

FIG. 3. Experimental results on the effect of periodic hydrophobic regions on mixing in a straight 7 mm microchannel. Normalized mixing index 0.5 signifies separated flow, and mixing index 0 signifies homogeneous mixing.

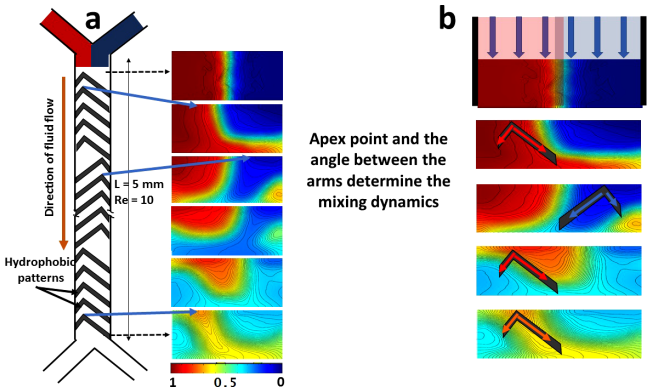

FIG. 4. Effect of periodic hydrophobic regions on mixing in a straight microchannel. (a) The asymmetric herringbone shaped hydrophobic regions introduce difference of resistance to flow along the arms of the asymmetric V shapes. (b) A zoomed version of one of these regions on the right shows the path of the fluid that flows over the patches. One can think of the Herringbone structures as irregular V shapes. Here, the vertices of the irregular V shapes introduce stagnation points in the fluid as we will clearly see later in Fig. 6. The arms of the hydrophobic patches introduce difference in flow resistance in comparison with the no-slip regions leading to recirculation in the flow. However, as the vertices of the asymmetric V shapes change location depending on the wavelength of the pattern, stagnation points of the recirculations also move back and forth, in turn introducing chaotic advection in the flow. The color bar in the figure shows the variation of concentration with red (1) as the concentration of the Allura Red solution and blue (0) as pure water. Simulation snapshots on the left are taken at locations starting at the inlet followed by every 1 mm downstream.

create a transverse pressure gradient generated through the difference of uneven flow resistances due to the inhomogeneity of the flow boundary conditions about the centerline. As can be seen from Fig. 1, the hydrophobic dots used in the experiments are not perfectly circular. This is expected as these dots were created manually using a black

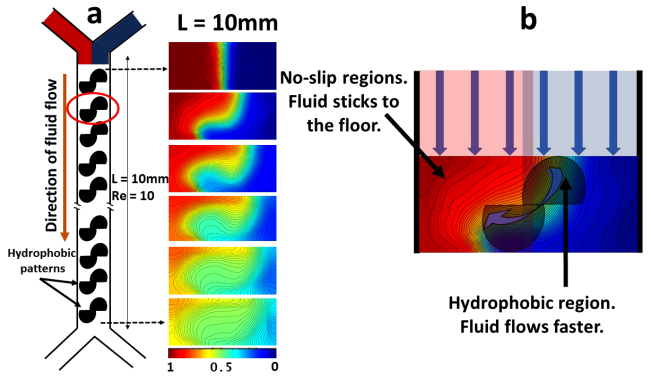

FIG. 5. Effect of periodic hydrophobic regions on mixing in a straight microchannel. (a) The asymmetric duck-shape hydrophobic regions introduce difference of resistance to the flow about the centerline of the channel. (b) A zoomed version of one of the hydrophobic regions shows the possible path of the fluid that flows over the shapes. It is clear that this pattern forces the fluids to bend the fluid, and one component of the fluid intrudes the other, thereby introducing effective transverse rotation and stretching and folding of the fluid volume as it flows downstream. Simulation snapshots on the left are taken at locations starting at the inlet followed by every 2 mm downstream.

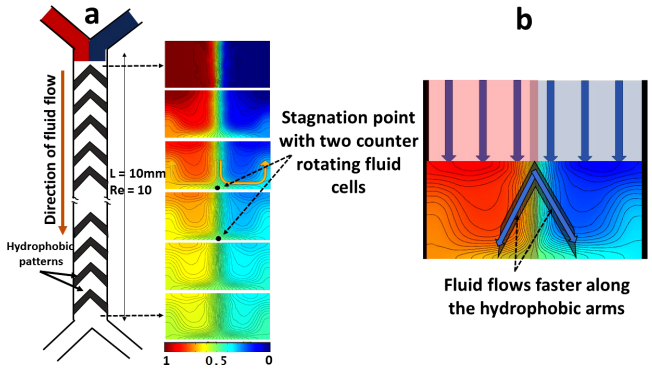

FIG. 6. Effect of periodic hydrophobic regions on mixing in a straight microchannel through symmetric V shapes hydrophobic patches. (a) The symmetric V shaped regions introduce difference of resistance to flow along the arms. (b) A zoomed version of one of the hydrophobic regions shows the path of the fluid that flows along the arms. An important observation is that the vertex of the V shape divides the flow and channel them obliquely in two opposite directions, thus creating counter rotating recirculation zones. Simulation snapshots on the left are taken at locations starting at the inlet followed by every 2 mm downstream.

sharpie marker. We have done simulations with perfectly circular hydrophobic dots; however, numerical results do not show significant mixing with those perfectly symmetrical circular dots. This is why we created duck shaped hydrophobic regions to break the symmetry and then simulation showed significant mixing behavior. Hence, we can conclude that asymmetry in the hydrophobic patterns plays an important role in mixing.

We argue that the floor of the channels is no-slip everywhere except the locations where there is a hydrophobic film. Thus, the hydrophobic regions on the floor apply less resistance to the fluid flow in comparison with the corresponding no slip region on the other side of the centerline. Each of the patterns, thus, may direct one component fluid (in our case could be blue) to intrude into the other (red), eventually creating a twisting, stretching, and folding of both the components as the fluids flow downstream and leading to a Smale horseshoe type mixing pathway as seen in Fig. 5.

Another pathway of mixing is found by creating counter rotating recirculation zones with the help of "V" shaped hydrophobic patterns (Fig. 6). It is clear that the stagnation point between the recirculating fluids aligns with the position of the apex point of the V shape. This feature is evident in the herringbone pattern (Fig. 4) also, where the stagnation points can be shifted periodically in the transverse direction by moving the apex points of the asymmetric V shapes. This creates different recirculation patterns as the fluids flow downstream leading toward effective mixing through chaotic advection. To check whether this enhanced mixing is a signature of deterministic chaos or not, we investigated the power-law dependence of the mixing length on the Péclet number *Pe*. When mixing occurs only via diffusion, the channel length required for mixing is given by $l_{mix} \sim Ut_{diff} \sim Ul^2/D \sim lPe$, whereas if there is a chaotic root to mixing via stretching and folding of liquid volumes over the cross section of the channel, then the mixing length would vary as $l_{mix} \sim l\ln(Pe)$.[19,25,26] A linear profile of l_{mix} with respect to $\ln(Pe)$ can, thus, be considered as a signature of chaotic advection in the system. In Fig. 7, we have indeed seen this behavior in our irregular V shaped passive microfluidic mixers.

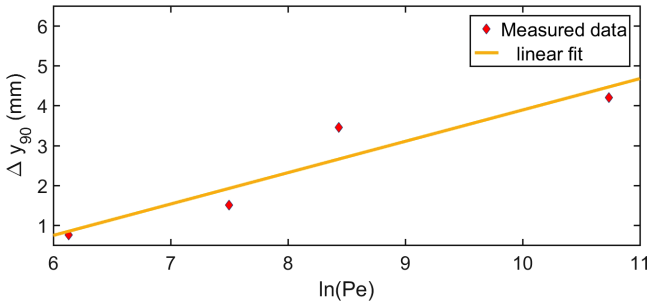

FIG. 7. Effect of Peclet number on mixing in a Herringbone mixer. A linear relationship between ln(Pe) and the mixing length, where 90% of mixing occurs indicates route to chaos[19] in a low Re environment. In the case of Duck shaped or symmetric V shaped mixers, mixing length varied nonlinearly with ln(Pe).

We were also curious to see if we can create a superposition of the Magnus type bending with the recirculating cells using both the pathways mentioned above, and the results are shown in Fig. 8. It shows that alternating twisting and recirculation gives rise to excellent mixing in the low Reynolds number laminar flow in a straight microchannel.

In Fig. 9, we show that even at Re = 0.1, Duck shape and symmetric V shaped hydrophobic patches can lead to significant mixing at the outlet of a 10 mm channel. Mixing index in numerical solutions is calculated using the same method as described in Ref. 19.

In conclusion, we claim that rapid mixing in low Reynolds number flow even in a straight microchannel can be achieved by manipulating twisting, stretching, and recirculation in the flow created by passive interventions through carefully chosen hydrophobic patterns on the walls/floor of the microchannels. In this easy and inexpensive

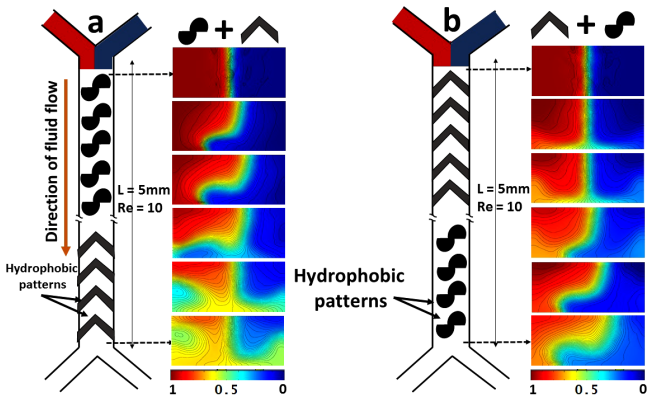

FIG. 8. Effect of periodic hydrophobic regions on mixing in a straight microchannel through hybrid patterns. We have observed a superposition of effects of stretching through rotation (by duck shapes) and recirculation (by V shapes) or vice versa. (a) Here, the duck shape patterns were created first close to the inlet followed by V shape patterns. It is clear that one component of the fluid intrudes into the other and introduces stretching and folding by the duck shape as discussed earlier. On top of that the symmetric V shapes create recirculating flow patterns leading toward complex mixing effect. (b) An opposite effect is observed when the pattern is switched, i.e., V shapes followed by the duck shapes. Recirculation followed by stretching and folding gives rise to a different mixed state. Simulation snapshots on the left are taken at locations starting at the inlet followed by every 1 mm downstream.

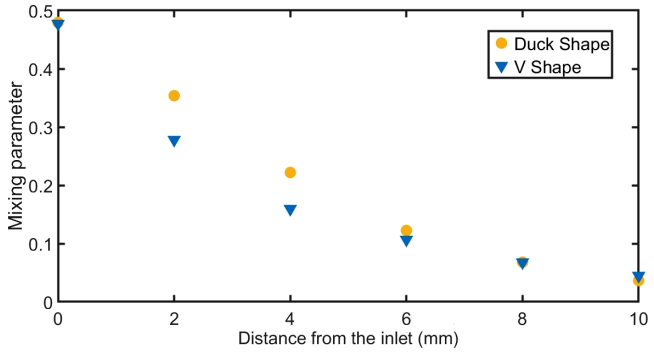

FIG. 9. Mixing index as a function of distance of slip patches from the inlet is shown for Duck shapes and symmetric V shapes. The graphs show near homogeneous mixing at the outlet of a 10 mm channel at Re = 0.1.

method, we would not even need complex three dimensional micro-/nano-patterning to create precise grooves and ridges on the floor of the channels[19] to introduce chaos, rather mixing can be manipulated by drawing hydrophobic no-slip spots on the floor of the channel by drawing the patterns with hydrophobic solutions/inks. This Letter may lead the microfluidic industry to an easy and inexpensive fabrication process to achieve efficient homogeneous mixing with a small mixing length scale.

ACKNOWLEDGMENTS

This work was partially supported by the National Science Foundation (HBCU-UP Award No. 1719425), the Department of Education (MSEIP Award No. P120A70068) with a MSEIP CCEM Supplemental award, and the Maryland Technology Enterprise Institute through a MIPS grant. K.D. would like to thank Dr. Jim Marty of the Minnesota Nano-Science Center and NanoLink for providing support and materials for the photolithography process in the microchannel fabrication.

AUTHOR DECLARATIONS

Conflict of Interest

The authors have no conflicts to disclose.

DATA AVAILABILITY

The data that support the findings of this study are available from the corresponding author upon reasonable request.

REFERENCES

[1]G. M. Whitesides, "The origins and the future of microfluidics," Nature **442**, 368 (2006).
[2]J.-L. Fraikin, T. Teesalu, C. M. McKenney, E. Ruoslahti, and A. N. Cleland, "A high-throughput label-free nanoparticle analyser," Nat. Nanotechnol. **6**, 308 (2011).
[3]D. Sinton, "Energy: The microfluidic frontier," Lab Chip **14**, 3127 (2014).
[4]D. Mark, S. Haeberle, G. Roth, F. Von Stetten, and R. Zengerle, "Microfluidic lab-on-a-chip platforms: Requirements, characteristics and applications," in *Microfluidics Based Microsystems* (Springer, 2010), pp. 305–376.
[5]M. Srisa-Art, A. J. Demello, and J. B. Edel, "Fluorescence lifetime imaging of mixing dynamics in continuous-flow microdroplet reactors," Phys. Rev. Lett. **101**, 014502 (2008).

[6]E. K. Sackmann, A. L. Fulton, and D. J. Beebe, "The present and future role of microfluidics in biomedical research," Nature **507**, 181 (2014).
[7]A. W. Martinez, S. T. Phillips, G. M. Whitesides, and E. Carrilho, "Diagnostics for the developing world: Microfluidic paper-based analytical devices," Anal. Chem. **82**, 3–10 (2010).
[8]S.-Y. Teh, R. Lin, L.-H. Hung, and A. P. Lee, "Droplet microfluidics," Lab Chip **8**, 198 (2008).
[9]K. Ando, A.-Q. Liu, and C.-D. Ohl, "Homogeneous nucleation in water in microfluidic channels," Phys. Rev. Lett. **109**, 044501 (2012).
[10]K. N. Nordstrom, E. Verneuil, P. Arratia, A. Basu, Z. Zhang, A. G. Yodh, J. P. Gollub, and D. J. Durian, "Microfluidic rheology of soft colloids above and below jamming," Phys. Rev. Lett. **105**, 175701 (2010).
[11]D. J. Collins, R. O'Rorke, C. Devendran, Z. Ma, J. Han, A. Neild, and Y. Ai, "Self-aligned acoustofluidic particle focusing and patterning in microfluidic channels from channel-based acoustic waveguides," Phys. Rev. Lett. **120**, 074502 (2018).
[12]S. Nagrath, L. V. Sequist, S. Maheswaran, D. W. Bell, D. Irimia, L. Ulkus, M. R. Smith, E. L. Kwak, S. Digumarthy, A. Muzikansky *et al.*, "Isolation of rare circulating tumour cells in cancer patients by microchip technology," Nature **450**, 1235 (2007).
[13]T. P. Burg, M. Godin, S. M. Knudsen, W. Shen, G. Carlson, J. S. Foster, K. Babcock, and S. R. Manalis, "Weighing of biomolecules, single cells and single nanoparticles in fluid," Nature **446**, 1066 (2007).
[14]E. Locatelli, M. Pierno, F. Baldovin, E. Orlandini, Y. Tan, and S. Pagliara, "Single-file escape of colloidal particles from microfluidic channels," Phys. Rev. Lett. **117**, 038001 (2016).
[15]P. S. Dittrich and A. Manz, "Single-molecule fluorescence detection in microfluidic channels—The holy grail in μTAS?," Anal. Bioanal. Chem. **382**, 1771 (2005).
[16]I. C. Christov, R. M. Lueptow, and J. M. Ottino, "Stretching and folding versus cutting and shuffling: An illustrated perspective on mixing and deformations of continua," Am. J. Phys. **79**, 359 (2011).
[17]S. Wiggins and J. M. Ottino, "Foundations of chaotic mixing," Philos. Trans. R. Soc. London, Ser. A **362**, 937 (2004).
[18]H. Aref, "Stirring by chaotic advection," J. Fluid Mech. **143**, 1–21 (1984).
[19]A. D. Stroock, S. K. Dertinger, A. Ajdari, I. Mezić, H. A. Stone, and G. M. Whitesides, "Chaotic mixer for microchannels," Science **295**, 647 (2002).
[20]S. Khodaparast, F. Boulogne, C. Poulard, and H. A. Stone, "Water-based peeling of thin hydrophobic films," Phys. Rev. Lett. **119**, 154502 (2017).
[21]Y. Xia and G. M. Whitesides, "Soft lithography," Annu. Rev. Mater. Sci. **28**, 153 (1998).
[22]B. K. Barnes, H. Ouro-Koura, J. Derickson, S. Lebarty, J. Omidokun, N. Bane, O. Suleiman, E. Omagamre, M. J. Fotouhi, A. Ogunmolasuyi *et al.*, "Plasma generation by household microwave oven for surface modification and other emerging applications," Am. J. Phys. **89**, 372 (2021).
[23]S. Bhattacharya, A. Datta, J. M. Berg, and S. Gangopadhyay, "Studies on surface wettability of poly(dimethyl) siloxane (PDMS) and glass under oxygen-plasma treatment and correlation with bond strength," J. Microelectromech. Syst. **14**, 590 (2005).
[24]H. Barkla and L. Auchterlonie, "The magnus or robins effect on rotating spheres," J. Fluid Mech. **47**, 437 (1971).
[25]J. M. Ottino, *The Kinematics of Mixing: Stretching, Chaos, and Transport* (Cambridge University Press, 1989), Vol. 3.
[26]S. W. Jones, O. M. Thomas, and H. Aref, "Chaotic advection by laminar flow in a twisted pipe," J. Fluid Mech. **209**, 335 (1989).